

# A new methodology for the determination of the workspace of six-DOF redundant parallel structures actuated by nine wires

Carlo Ferraresi<sup>\*†</sup>, Marco Paoloni<sup>‡</sup> and Francesco Pescarmona<sup>†</sup>

<sup>†</sup>Dipartimento di Meccanica, Politecnico di Torino, Corso Duca degli Abruzzi, 24, Torino 10129, Italy.

<sup>‡</sup>Robotic Section of the Nuclear Fusion Unit, ENEA C.R. Casaccia, Via Anguillarese, 301, Roma 00060, Italy.

(Received in Final Form: July 27, 2006, First published online: October 12, 2006)

## SUMMARY

The WiRo-6.3 is a six-degrees of freedom (six-DOF) robotic parallel structure actuated by nine wires, whose characteristics have been thoroughly analyzed in previous papers in reference<sup>2</sup>. It is thought to be a master device for teleoperation; thus, it is moved by an operator through a handle and can convey a force reflection on the operator's hand. A completely new method for studying the workspace of this device, and of virtually any nine-wire parallel structure actuated by wire is presented and discussed, and its results are given in a graphical form.

KEYWORDS: Parallel robot; workspace; wire actuation.

## 1. Introduction

Mechanical structures actuated by wires (wire robots) are characterized by the presence of a mobile platform (representing the end-effector) connected by several wires to a fixed frame; the wires are fixed to the platform, rolled over pulleys and stretched by motors fixed to the frame in order to exert forces and torques. At the same time, the position and orientation of the mobile platform can be determined by the measured wire lengths. Wire robots are parallel devices having wires as links, and belong to a set of fully parallel structures because every wire is an independent chain with one DOF.<sup>1, 4–6</sup>

With respect to the traditional parallel structures, wire-actuated robots have several advantages: they allow great manoeuvrability, thanks to a reduced mass, and also promise lower costs with respect to traditional actuators. Furthermore, the stroke length of each linear joint does not follow the same restrictions as with conventional structures, because wires can be extended to much higher lengths, unwinding from a spool. This kind of a structure allows to comply with several needs in applications where conventional manipulation technology can be hardly used for technical or economical reasons. We could mention, for example, crane robots,<sup>1, 4</sup> high-speed manipulation robots<sup>5</sup> and force feedback devices to be used as masters in master–slave teleoperation systems.<sup>6</sup>

Such devices offer many advantages, such as a simplified mechanical structure, very high speed, relatively large workspace and low inertia. However, it must be noted that wires can only pull objects and not push on them: this unilateral constraint compels the adoption of a redundant actuating mechanism. This can be seen as an analogy with the grasping problem for multi-finger systems with frictionless point contact; the forces exerted by the fingers on the grasped object are subject to the same unidirectional constraint.

It has been stated<sup>5, 6, 9, 13</sup> that to obtain  $n$  degrees of freedom (DOFs) without external forces (or the gravity in the crane case) it is necessary and sufficient to use  $n + 1$  wires; These devices are usually referred to as completely restrained position mechanism (CRPM), while devices with a higher number of wires are referred to as redundantly restrained position mechanism (RRPM).

The study of the operative characteristics of wire-driven devices may present more difficulties than the traditional ones, in particular for the definition of their workspace and dexterity. The workspace is not simply the set of non-singular platform positions and orientations compatible with the joints limits, but it is also necessary that all forces and torques exerted in such platform poses should be obtainable only by means of a set of wire forces directed from the platform to the frame. Furthermore, the shape and the dimensions of the workspace, and the dexterity of these devices are greatly influenced by the number of wires and their geometrical disposition.

It has been stated by several authors<sup>5, 6, 12, 13</sup> that in a certain pose of the end-effector of a six-DOF mechanism driven by  $m$  wires, it is possible to exert arbitrary force and moment, if and only if, the transpose of the inverse Jacobian (called the *structure matrix* with six rows and  $m$  columns) has a rank equal to six and if it is possible to find a vector belonging to its null space with all the components strictly positive. Practically speaking, after the evaluation of the null space base constituted by  $m - 6$  vectors with  $m$  components, to decide if the considered pose belongs to the workspace at least one set of  $m - 6$  coefficients must be found to form a linear combination of the  $m - 6$  base vectors yielding a resultant with all the  $m$  components strictly positive.

For the CRPM case ( $m = 7$ ), the null space is a one-dimensional (1-D) space vector and then the examined pose belongs to the workspace if the vector chosen as base of the null space has all the seven components of the same sign. For

\*Corresponding author. E-mail: carlo.ferraresi@polito.it

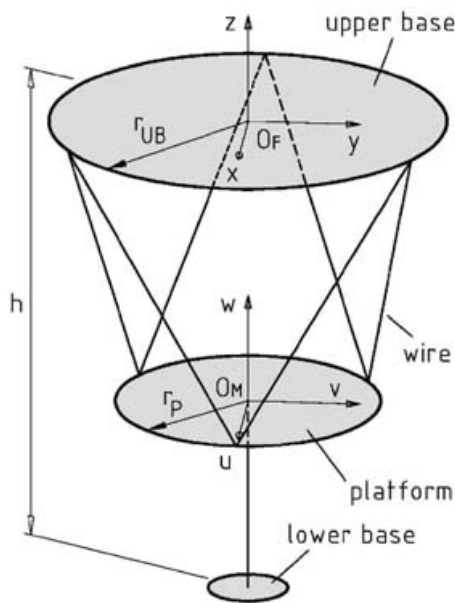


Fig. 1. The WiRo-6.1 structure.

the RRPM case ( $m > 7$ ), the null space examination is not trivial and solutions can be found using algorithms like the ones used in linear programming problems of constrained optimization.<sup>13</sup>

In the Department of Mechanics of the Politecnico di Torino and in the Robotics Section of the ENEA, researches on wire parallel structures have been carried out in order to identify appropriate analysis and design criteria for the development of devices devoted to remote manipulation and sensed teleoperation.

Starting from a number of seven-wire structures, which is the minimum number of wires able to provide six-DOFs, some analysis methodologies were implemented and adopted, such as the use of appropriate indexes to identify the best performing structures through an objective evaluation of their workspaces.<sup>3</sup> As a first result, one seven-wire structure, WiRo-6.1 (Fig. 1), was chosen as the starting point for future development, although its main problems were a very small workspace and low dexterity.

Then, a new structure was conceived in order to lessen the disadvantages of the earlier structure. The lower, single wire was replaced by three wires converging in  $O_M$ , thus obtaining a highly redundant structure with a large workspace, good dexterity and a better equilibrium in the disposal of wires. This structure was called WiRo-6.3, and its inverse and forward kinematics were both solved in a closed form.<sup>2</sup>

In this paper, a novel analytical methodology is proposed for identifying the workspace of a nine-wire redundant structure. In particular, this procedure was applied to the study of WiRo-6.3, demonstrating that it possesses a larger workspace and a more dexterous behavior than WiRo-6.1.

## 2. Workspace Definition

Together with the properties of the structure matrix, in the study of the workspace of wire robots further aspects must be considered:<sup>11</sup> the structure must be sufficiently stiff, wires must not intersect with each other and with the environment and the stretching tension must lie between a minimum (in

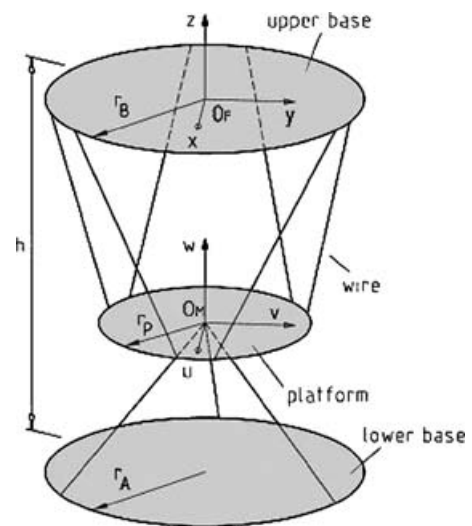


Fig. 2. The WiRo-6.3 structure.

order to prevent wires becoming slack) and a maximum value (determined by the motors, the breaking loads of the wires, etc.).

These aspects are not considered in this paper because they pertain to the practical realization of the mechanisms, while the objective of our work is the development of a procedure to explore the theoretical limits of these structures. The workspaces obtained in this condition are called *controllable workspaces*, while those obtained with all aspects considered are called *feasible workspaces*; usually a feasible workspace is a subset of the correspondent controllable workspace.

In the following sections, geometrical and analytical considerations will lead to a procedure to calculate whether a platform pose belongs to the workspace or not. Since it is difficult to obtain a closed-form description of the workspaces of such robots, they are described as grids of points, starting from a discrete subdivision of the internal volume of the fixed frame.

As can be seen in Figs. 1 and 2, the groups of six wires of both WiRo-6.1 and WiRo-6.3 devices are disposed as the actuators of a Stewart-Gough platform, a well-known parallel mechanism with an amount of technical bibliography.<sup>17</sup> The workspaces of this and similar devices have been widely studied<sup>17–22</sup> using different methodologies from the analytical study of the zeroes of its Jacobian determinant<sup>18, 19</sup> to the application of the Lie algebra.<sup>20</sup>

All these studies, though, can bring a relatively poor contribution to our work because they do not deal with the problem of the unilateral actuation of the wires, they can be used to evaluate the rank of the structure matrix; in fact, it can be recognized that the limitations to the platform motion imposed by the need of preventing wire tangles constraints the dispositions of the group of six wires in non-singular configurations of a correspondent Stewart-Gough platform. In this way, the block of the structure matrix associated with the six wires group is a  $6 \times 6$  matrix with non-null determinant, ensuring the full rank of the whole structure matrix and allowing to concentrate on its null space examination.

### 3. Force Closure

The force closure of a parallel structure in a particular configuration can be expressed as

$$-\mathbf{W} = \mathbf{f} = \tilde{\mathbf{J}} \cdot \boldsymbol{\tau} \tag{1}$$

where, in the case of a nine-wire parallel robot,  $\mathbf{W}$  is the six-component wrench acting on the platform,  $\mathbf{f}$  is the wrench provided by the robot,  $\tilde{\mathbf{J}}$  is the  $6 \times 9$  structure matrix evaluated over any particular configuration and  $\boldsymbol{\tau}$  is the nine-component vector containing the tensions of the wires.

The condition representing the belonging of a given pose to the workspace can be expressed imposing that for any  $\mathbf{f}$  the tensions of the wires can all be made positive (or greater than a prefixed positive value)

$$\boldsymbol{\tau} > 0. \tag{2}$$

Since  $\tilde{\mathbf{J}}$  is not square, among the infinite solutions of Eq. (1) for any given  $\mathbf{f}$ , the minimum-norm solution can be obtained by means of the pseudoinverse

$$\boldsymbol{\tau}_{\min} = \tilde{\mathbf{J}}^+ \cdot \mathbf{f} \tag{3}$$

where  $\tilde{\mathbf{J}}^+$  is the pseudoinverse of  $\tilde{\mathbf{J}}$ .

The generic solution of Eq. (1) is given by

$$\boldsymbol{\tau} = \boldsymbol{\tau}_{\min} + \boldsymbol{\tau}^* \tag{4}$$

where  $\boldsymbol{\tau}^*$  must belong to the null space of  $\tilde{\mathbf{J}}$

$$\tilde{\mathbf{J}} \cdot \boldsymbol{\tau}^* = 0. \tag{5}$$

This means that the infinite possible values of  $\boldsymbol{\tau}$  can be found by adding to  $\boldsymbol{\tau}_{\min}$  a set of vectors that do not affect the resulting wrench.

Equation (2) may be reached imposing that for each point of the workspace at least a strictly positive  $\boldsymbol{\tau}^*$  exists, satisfying Eq. (5). In this way, knowing that all its multiples also belong to the null space of  $\tilde{\mathbf{J}}$ , it is possible to find an appropriate positive multiplier  $c$  capable of compensating the negative components of  $\boldsymbol{\tau}_{\min}$

$$\mathbf{f} = \tilde{\mathbf{J}}(\boldsymbol{\tau}_{\min} + c \cdot \boldsymbol{\tau}^*) \tag{6}$$

where

$$c \cdot \boldsymbol{\tau}^* \in \text{null}(\tilde{\mathbf{J}}); \quad \boldsymbol{\tau}_{\min} + c \cdot \boldsymbol{\tau}^* > 0.$$

### 4. Workspace Analysis

The procedure for the analysis of the workspace consists of studying a discretized six-dimensional (6-D) space comprising three displacements and three rotations, point by point, checking whether the rank of  $\tilde{\mathbf{J}}$  is maximum (equal to 6) and a strictly positive  $\boldsymbol{\tau}^*$  exists, satisfying Eq. (5).

If  $n$  is the number of degrees of freedom of a structure, and  $m$  is the number of its actuators, the base of the null space of  $\tilde{\mathbf{J}}$  (if  $\tilde{\mathbf{J}}$  has rank  $n$ ) is a set of  $m - n$  vectors, each with  $m$  components.

In the case of a nine-wire robot, the base of the null space of  $\tilde{\mathbf{J}}$  is composed by three nine-component vectors, a linear combination of which may provide the desired  $\boldsymbol{\tau}^*$ .

Naming  $[\mathbf{ker}] \in R^{9 \times 3}$  the matrix whose columns generate the null space of  $\tilde{\mathbf{J}}$ ,  $\boldsymbol{\tau}^*$  can be written as a linear combination

of its columns. Equation (2), considering Eq. (5) as well, can be expressed by the following inequality:

$$\boldsymbol{\tau}^* = [\mathbf{ker}] \times \begin{bmatrix} \alpha \\ \beta \\ \gamma \end{bmatrix} > 0 \tag{7}$$

where  $\alpha$ ,  $\beta$  and  $\gamma$  are three unknown quantities.

Developing Eq. (7) yields

$$\begin{cases} k_{11}\alpha + k_{12}\beta + k_{13}\gamma > 0 \\ k_{21}\alpha + k_{22}\beta + k_{23}\gamma > 0 \\ k_{31}\alpha + k_{32}\beta + k_{33}\gamma > 0 \\ k_{41}\alpha + k_{42}\beta + k_{43}\gamma > 0 \\ k_{51}\alpha + k_{52}\beta + k_{53}\gamma > 0 \\ k_{61}\alpha + k_{62}\beta + k_{63}\gamma > 0 \\ k_{71}\alpha + k_{72}\beta + k_{73}\gamma > 0 \\ k_{81}\alpha + k_{82}\beta + k_{83}\gamma > 0 \\ k_{91}\alpha + k_{92}\beta + k_{93}\gamma > 0 \end{cases} \tag{8}$$

where  $k_{ij}$  are the components of  $[\mathbf{ker}]$ .

Observing Eq. (8) shows that either it has no solution, or in the three-dimensional (3-D) space generated by  $\alpha$ ,  $\beta$  and  $\gamma$  it determines a polyhedral angle with vertex in the origin and polygonal cross section (Fig. 3).

In case no solution of Eq. (8) exists, the corresponding positioning point does not belong to the workspace; on the contrary, if the polyhedral angle exists, there is an infinite number of sets  $(\alpha, \beta, \gamma)$  satisfying Eq. (8), and they are all contained inside the polyhedral angle. This means that any external wrench can be compensated by positive tensions in the wires, and so the positioning point belongs to the workspace. Sectioning the polyhedral angle with a cylinder coaxial with  $\alpha$ , considering cylindrical coordinates with  $\theta$  as the angle on the plane  $\beta\gamma$ , something analogous to Fig. 4 is obtained.

Combining linearly the three columns of  $\tilde{\mathbf{J}}$ , it is always possible to determine a new base of the null space of  $\tilde{\mathbf{J}}$  such

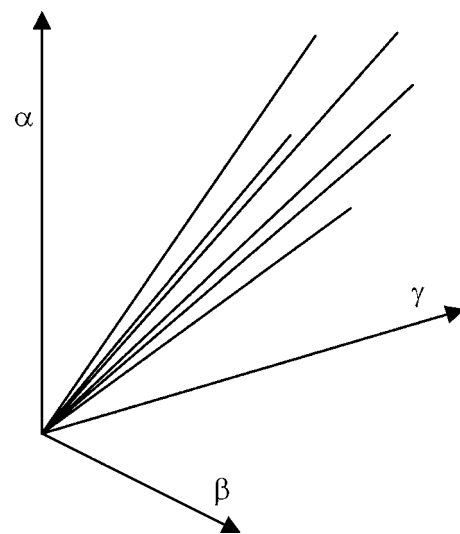


Fig. 3. The polyhedral angle determined by inequations given in Eq. (8).

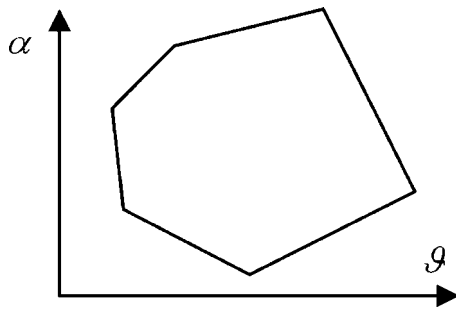


Fig. 4. A generic section of the polyhedral angle.

that its last three rows are

$$\begin{bmatrix} 1 & 0 & 0 \\ 0 & 1 & 0 \\ 0 & 0 & 1 \end{bmatrix}$$

thus limiting the search to the portion of space in which  $\alpha$ ,  $\beta$  and  $\gamma$  are all greater than zero.

Naturally, the other elements of  $[\mathbf{ker}]$  will change consequently. The new matrix will be called  $[\mathbf{ker}^*]$  to highlight the modification performed.

The last three rows of  $[\mathbf{ker}^*]$  now represent the conditions

$$\begin{cases} \alpha > 0 \\ \beta > 0 \\ \gamma > 0. \end{cases} \quad (9)$$

The first six rows of  $[\mathbf{ker}^*]$  may be written in the form

$$\begin{aligned} \alpha &> -\frac{k_{i2}\beta + k_{i3}\gamma}{k_{i1}}, & \text{if } k_{i1} > 0 \\ \alpha &< -\frac{k_{i2}\beta + k_{i3}\gamma}{k_{i1}}, & \text{if } k_{i1} < 0 \end{aligned} \quad (10)$$

for  $i = 1$  to  $6$ .

If  $k_{i1}$  is null, the inequations are

$$\begin{aligned} \frac{\gamma}{\beta} &> -\frac{k_{i2}}{k_{i3}}, & \text{if } k_{i3} > 0 \\ \frac{\gamma}{\beta} &< -\frac{k_{i2}}{k_{i3}}, & \text{if } k_{i3} < 0 \end{aligned} \quad (11)$$

for  $i = 1$  to  $6$ .

In this case, it is not important to exclude the case when  $k_{i3}$  is zero, because the ratio  $\gamma/\beta$  may be infinite, as will be pointed out afterwards.

The first and the second inequations of Eq. (10) express respectively, the lower and upper limits for the values of  $\alpha$ , as a function of the coefficients  $k_{ij}$  and of the value of  $\beta$  and  $\gamma$ . The lower limits are counted through the letter  $l = 1, \dots, l^*$ , while the upper limits are counted through the letter  $u = 1, \dots, u^*$ .

For at least one valid  $\alpha$  to exist, every lower limit must be smaller than every upper limit, which is equivalent

to applying

$$-\frac{k_{l2}\beta + k_{l3}\gamma}{k_{l1}} < -\frac{k_{u2}\beta + k_{u3}\gamma}{k_{u1}} \quad \text{for } l = 1, \dots, l^*, \quad u = 1, \dots, u^* \quad (12)$$

for each possible combination between a lower limit and a upper limit as from Eq. (10). Moreover, the first condition of Eq. (9), requiring  $\alpha > 0$ , means that all the upper limits must be greater than zero

$$-\frac{k_{u2}\beta + k_{u3}\gamma}{k_{u1}} > 0, \quad \text{for } u = 1, \dots, u^* \quad (13)$$

for every upper limit as from Eq. (10).

Remembering that  $\beta > 0$  as per Eq. (9), Eq. (12) may be written as

$$\begin{aligned} \frac{\gamma}{\beta} &> \frac{\left(\frac{k_{u2}}{k_{u1}} - \frac{k_{l2}}{k_{l1}}\right)}{\left(\frac{k_{l3}}{k_{l1}} - \frac{k_{u3}}{k_{u1}}\right)}, & \text{if } \left(\frac{k_{l3}}{k_{l1}} - \frac{k_{u3}}{k_{u1}}\right) > 0 \\ \frac{\gamma}{\beta} &< \frac{\left(\frac{k_{u2}}{k_{u1}} - \frac{k_{l2}}{k_{l1}}\right)}{\left(\frac{k_{l3}}{k_{l1}} - \frac{k_{u3}}{k_{u1}}\right)}, & \text{if } \left(\frac{k_{l3}}{k_{l1}} - \frac{k_{u3}}{k_{u1}}\right) < 0. \end{aligned} \quad (14)$$

If  $\left(\frac{k_{l3}}{k_{l1}} - \frac{k_{u3}}{k_{u1}}\right) = 0$ , no problem occurs, since  $\gamma/\beta$  may be infinite as will be better explained in the following sections. The possibility that both the numerator and the denominator are zero is excluded by the check of the rank of  $\tilde{\mathbf{J}}$ .

Equation (13) may be written as

$$\begin{aligned} \frac{\gamma}{\beta} &> \frac{-k_{u2}}{k_{u3}}, & \text{if } \frac{k_{u3}}{k_{u1}} < 0 \\ \frac{\gamma}{\beta} &< \frac{-k_{u2}}{k_{u3}}, & \text{if } \frac{k_{u3}}{k_{u1}} > 0. \end{aligned} \quad (15)$$

In the 3-D space generated by  $\alpha$ ,  $\beta$  and  $\gamma$ , the projection of the polyhedral angle (8) on the plane  $\beta\gamma$  determines an angle delimited by an interval  $[\theta_1, \theta_2]$ , as given in Fig. 5, where a generic  $\theta$  is represented as well. Remembering that

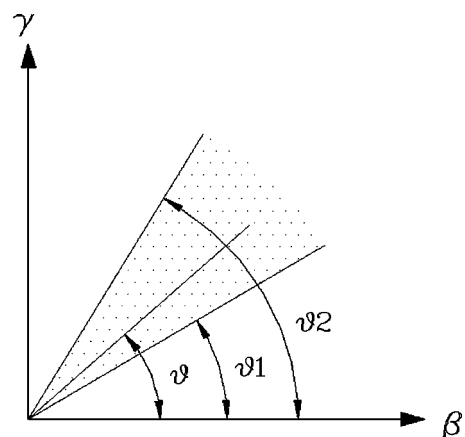


Fig. 5. Projection of the polyhedral angle on the plane  $\beta\gamma$ .

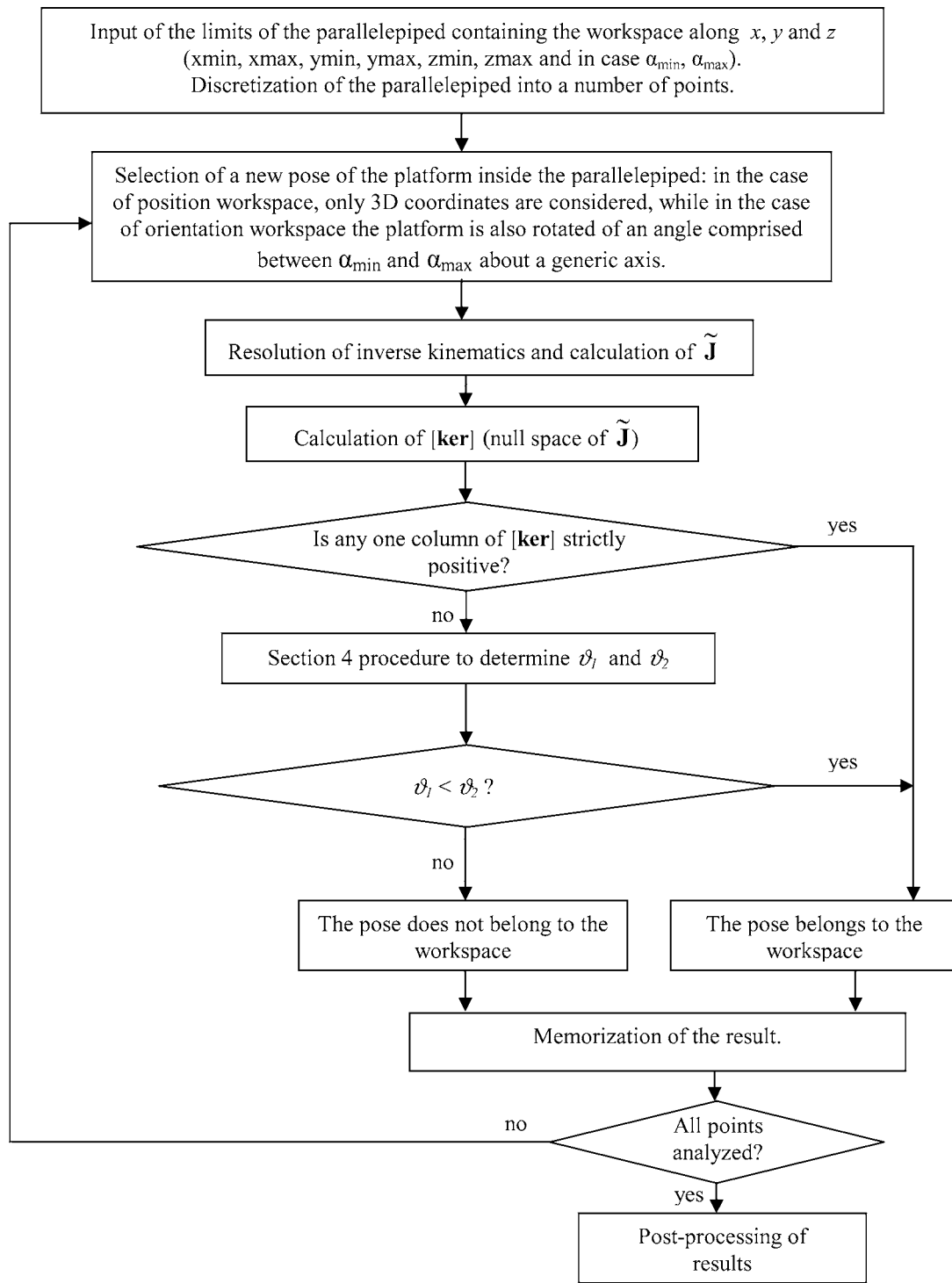


Fig. 6. Flowchart of the workspace-determination procedure.

$\beta > 0$  and  $\gamma > 0$  as per Eq. (9)

$$\begin{aligned} 0^\circ < \theta_1 < 90^\circ \\ 0^\circ < \theta_2 < 90^\circ. \end{aligned} \quad (16)$$

Now, imposing  $\beta = \cos \theta$  and  $\gamma = \sin \theta$ , the generic angle  $\theta$  can be expressed in the form

$$\theta = \text{atan} \frac{\gamma}{\beta}. \quad (17)$$

This explains why the ratio  $\gamma/\beta$  may be infinite: the corresponding angle  $\theta$  would be  $90^\circ$ .

In this notation, the inequations in Eqs. (11), (14) and (15) express the lower and the upper limits for  $\theta$  (note that the limitations of  $\alpha$  have been discussed previously). Therefore, considering the notation of Fig. 5 as well, let the greatest of the lower limits be  $\theta_1$ , and the smallest of the upper limits be  $\theta_2$

$$\begin{aligned} \theta_1 &= \max \left[ \text{atan} \left( \frac{\gamma}{\beta} \right) \right]_{l=1, \dots, l^*} \\ \theta_2 &= \min \left[ \text{atan} \left( \frac{\gamma}{\beta} \right) \right]_{u=1, \dots, u^*}. \end{aligned} \quad (18)$$

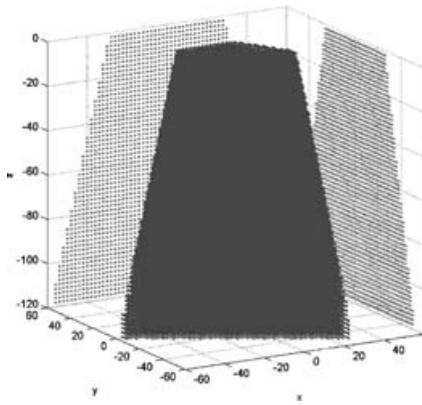


Fig. 7. WiRo-6.3: Positional workspace ( $r_{UB} = r_{LB} = 60$ ,  $r_P = 30$ ,  $h = 120$ ).

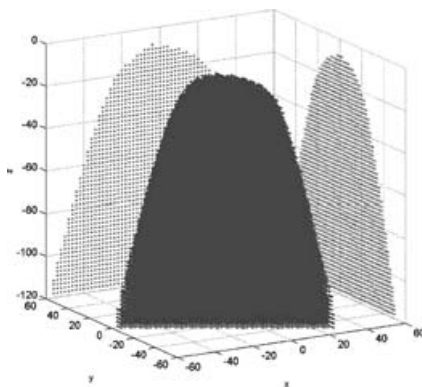


Fig. 8. WiRo-6.3: Orientation workspace ( $\alpha = 10^\circ$ ).

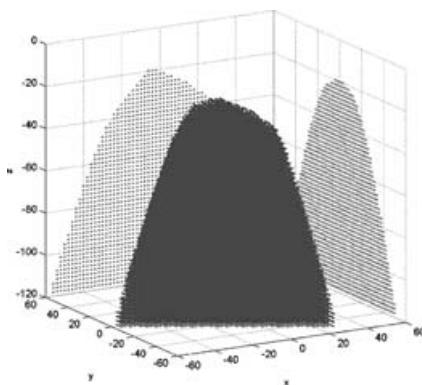


Fig. 9. WiRo-6.3: Orientation workspace ( $\alpha = 20^\circ$ ).

If  $\theta_1 < \theta_2$ , then there is a non-null angular interval on the plane  $\beta\gamma$ , which, being its projection, indicates the presence of the polyhedral angle [Eq. (8)], thus guaranteeing the existence of an infinite number of sets  $(\alpha, \beta, \gamma)$  satisfying Eq. (7). In this way, as pointed above, the tensions in the wires can in any case be made positive.

In conclusion, if  $\theta_1 < \theta_2$  then the particular 6-D point representing the position and orientation of the robot is part of the workspace; if this is not verified, it is discarded.

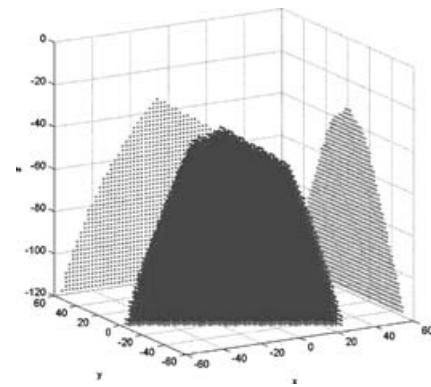


Fig. 10. WiRo-6.3: Orientation workspace ( $\alpha = 30^\circ$ ).

### 5. Practical Application of the Workspace-Determination Procedure

The algorithm of Section 4 can be used to determine whether a single platform pose (position and orientation) belongs to the workspace or not. Consequently, it must be part of a wider analysis strategy to identify the complete workspace of the nine-wire structure. According to figure 6 flowchart, the simplest thing is to consider a parallelepiped containing the device or at least the workspace. The parallelepiped can then be discretized according to the required accuracy level.

In order to obtain a useful graphical representation of the workspace, the orientation and position degrees of freedom can be considered separately, calling the whole of 3-D points with null orientation (i.e. with Euler angles  $\psi = 0$ ,  $\chi = 0$ ,  $\varphi = 0$ ) belonging to the 6-D workspace *positional workspace* as the, and the whole of 3-D points in which, considering a given angle  $\alpha$ , all combinations of  $\psi$ ,  $\chi$ ,  $\varphi$  resulting in a rotation around a generic axis of an angle smaller than or equal to  $\alpha$  belonging to the 6-D workspace as the  *$\alpha$ -orientation workspace*.

Therefore, in the case of the positional workspace only the displacement of the platform will be varied through all the discretized points along  $x$ ,  $y$  and  $z$ ; for every point, the full procedure of Section 4 will be applied in order to recognize whether the point belongs to the workspace or not. In the case of  $\alpha$ -orientation workspace, the analysis will anyway be conducted starting from the discretized positions, but for every position the orientation of the platform will be varied applying a discretized set of combinations of  $\psi$ ,  $\chi$ ,  $\varphi$  resulting in a rotation around a generic axis of an angle smaller than or equal to  $\alpha$ . For the sake of visualization, the 3-D point of the discretized parallelepiped will belong to the orientation workspace, if and only if, each and every considered combination of  $\psi$ ,  $\chi$ ,  $\varphi$  at that position has been found to be belonging to the 6-D workspace.

The method presented in the previous sections has been applied to several nine-wire structures. In particular, Figs. 7–10 show the positional workspace and three different orientation workspaces for WiRo-6.3 having a given structure geometry ( $r_{UB} = r_{LB} = 60$ ,  $r_P = 30$ ,  $h = 120$ ).

In all the figures, the central shape is a 3-D view of the workspace, while on the coordinate planes the projections of the workspace are shown. These results have been compared to those concerning the WiRo-6.1 structure having

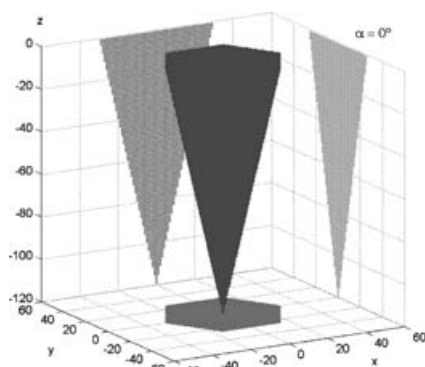
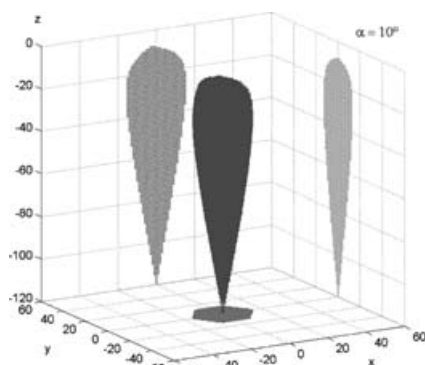
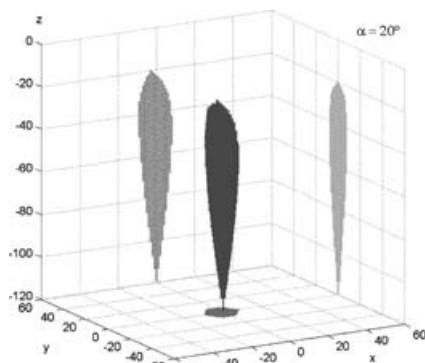


Fig. 11. WiRo-6.1: Positional workspace.

Fig. 12. WiRo-6.1: Orientation workspace ( $\alpha = 10^\circ$ ).Fig. 13. WiRo-6.1: Orientation workspace ( $\alpha = 20^\circ$ ).

the same geometrical dimensions. Figures 11–13 show the corresponding workspaces. By this comparison, it is immediately clear that WiRo-6.3 has a much larger workspace in all directions. The differences from its predecessor become particularly evident in the lower part, where WiRo-6.1 can only move within a very small portion of space. Furthermore, when the platform gets orientations different from zero, WiRo-6.3 maintains a noticeable manoeuvrability in the lower part, while WiRo-6.1 has a very thin orientation workspace. Even with  $\alpha = 30^\circ$ , which generated a minuscule volume for WiRo-6.1, WiRo-6.3 can be controlled in a certain zone of space.

From this example, it is evident that the capability of the proposed method to investigate both the positional and the orientation workspaces allows us to make a significant

analysis and comparison of the performance of different wire-actuated structures.

## 6. Conclusions

Although the analysis of the workspace of parallel structures has been studied extensively and has led to a number of analytical methods for investigation, such methods in general cannot be applied directly to wire-actuated structures, since their workspace depends not only on the structure geometry but also on the capability of the wires to exert only the traction forces. In this paper, a new method has been presented for the analysis of the workspace of wire parallel structures with triple redundancy. The method is useful to investigate both the positional and the orientation workspaces. It was developed for WiRo-6.3 but it can be applied to any nine-wire parallel robot and, with a few simplifications that can be easily derived from this paper, to seven- and eight-wire robots as well.

The results produced by the method allow us to make significant comparisons between different wire-actuated structures, showing the performance differences in a quantitative form.

## Acknowledgements

This work was partially funded by the Robotics and Telescience Research projects of the Italian Antarctic Research Programme (PNRA). The authors wish to thank the Italian Ministry of University and Research (MIUR) for their support.

## References

1. J. S. Albus, R. V. Bostelman and N. G. Dagalakis, "The NIST ROBOCRANE," *J. Robot. Syst.* **10**, 709–724 (1993).
2. C. Ferraresi, M. Paoloni, S. Pastorelli and F. Pescarmona, "A new 6-d.o.f. parallel robotic structure actuated by wires: The WiRo-6.3," *J. Robot. Syst.* **21**(11), 581–595 (2004).
3. C. Ferraresi, S. Pastorelli and F. Pescarmona, "Workspace analysis and design criteria of 6 d.o.f. wire parallel structures," *Proceedings of the 10th International Workshop on Robotics in Alpe-Adria-Danube Region, RAAD '01*, Vienna, Austria (May 16–18, 2001).
4. S. Havlik, "Cable Robotic Manipulators," *Proceedings of the 8th International Workshop on Robotics in Alpe-Adria-Danube Region, RAAD '99*, München, Germany (1999) pp. 303–308.
5. S. Kawamura, W. Choe, S. Tanaka and S. R. Pandian, "Development of an ultrahigh speed robot FALCON using wire drive system," *Proceedings of the IEEE International Conference on Robotics and Automation*, Nagoya, Japan (1995) pp. 215–220.
6. S. Kawamura and K. Ito, "A new type of master robot for teleoperation using a radial wire mechanism," *Proceedings of the IEEE/RSJ International Conference on Intelligent Robots and Systems*, Yokohama, Japan (1993) pp. 55–60.
7. C. A. Klein and C. H. Huang, "Review of pseudoinverse control for use with kinematically redundant manipulators," *IEEE Trans. Syst., Man, Cybern.* **SMC-13**(3), 245–250 (Mar.–Apr. 1983).
8. A. Liégeois, "Automatic supervisory control of the configuration and behavior of multibody mechanisms," *IEEE Trans. Syst., Man, Cybern.* **SMC-7**(12), 868–871 (Dec. 1997).
9. V. D. Nguyen, "Constructing force-closure grasps in 3D," *Proceedings of the 1987 IEEE International Conference on Robotics and Automation* (1987) pp. 240–245.

10. D. Stewart, "A platform with six degrees of freedom," *U.K. Inst. Mech. Eng. Proc.* **180**(1), 15, 371–386 (1966).
11. R. Verhoeven, M. Hiller and S. Tadokoro, "Workspace, stiffness, singularities and classification of tendon-driven Stewart platforms," *Adv. Robot Kinemat.: Anal. Control* 105–114 (1998).
12. A. Ming and T. Higuchi, "Study on multiple degree-of-freedom positioning mechanism using wires (Part 1)—Concept, design and control," *Int. J. Jpn. Soc. Prec. Eng.* **28**(2), 131–138 (1994).
13. R. G. Roberts, T. Graham and T. Lippitt, "On the inverse kinematics, statics, and fault tolerance of cable-suspended robots," *J. Robot. Syst.* **15**(10), 581–597 (1998).
14. E. F. Fichter, "A Stewart platform-based manipulator: General theory and practical construction," *Int. J. Robot. Res.* **5**(2), 157–182 (1986).
15. C. Gosselin and J. Angeles, "Singularity analysis of closed-loop kinematic chain," *IEEE Trans. Robot. Autom.* **6**(3), 281–290 (1990).
16. C. Gosselin, "Determination of the workspace of 6-dof parallel manipulators," *J. Mech. Des.* **112**, 331–336 (1990).
17. J. P. Merlet, "Determination of 6D workspaces of Gough-type parallel manipulator and comparison between different geometries," *Int. J. Robot. Res.* **18**(9), 902–916 (1999).
18. V. Parenti-Castelli, "Workspace and optimal design of a pure translation parallel manipulator," *Meccanica* **35**, 203 (2000).
19. V. Kumar, "Characterization of workspaces of parallel manipulators," *J. Mech. Des.* **114**, 368 (1992).
20. G. S. Chirikjian and I. Ebert-Uphoff, "Numerical convolution on the Euclidean group with applications to workspace generation," *IEEE Trans. Robot. Autom.* **14**(1), 123–136 (Feb. 1998).
21. A. Kosinska, M. Galicki and K. Kedzior, "Design of parameters of parallel manipulators for a specified workspace," *Robotica* **21**(5), 575–579 (Sep.–Oct. 2003).
22. S. Bhattacharya, H. Hatwal and A. Ghosh, "On the optimum design of Stewart platform type parallel manipulators," *Robotica* **13**(2), 133–140 (Mar.–Apr. 1995).